HHS Public Access

Author manuscript

Nature. Author manuscript; available in PMC 2011 November 02.

Published in final edited form as:

Nature. 2010 June 24; 465(7301): 1033–1038. doi:10.1038/nature09144.

A coding-independent function of gene and pseudogene mRNAs regulates tumour biology

Laura Poliseno[1,†,*], **Leonardo Salmena**[1,*], **Jiangwen Zhang**[2], **Brett Carver**[3], **William J. Haveman**[1], and **Pier Paolo Pandolfi**[1]

[1]Cancer Genetics Program, Beth Israel Deaconess Cancer Center, Departments of Medicine and Pathology, Beth Israel Deaconess Medical Center, Harvard Medical School, Boston, MA 02215

[2]FAS Center for Systems Biology, Harvard University, Cambridge, MA, 02138, USA

[3]Human Oncology and Pathogenesis Program, Department of Surgery, Memorial Sloan-Kettering Cancer Center, 1275 York Avenue, New York, NY, 10021

Abstract

The canonical role of messenger RNA (mRNA) is to deliver protein-coding information to sites of protein synthesis. However, given that microRNAs bind to RNAs, we hypothesized that RNAs possess a biological role in cancer cells that relies upon their ability to compete for microRNA binding and is independent of their protein-coding function. As a paradigm for the protein-coding-independent role of RNAs, we describe the functional relationship between the mRNAs produced by the *PTEN* tumour suppressor gene and its pseudogene (*PTENP1*) and the critical consequences of this interaction. We find that *PTENP1* is biologically active as determined by its ability to regulate cellular levels of PTEN, and that it can exert a growth-suppressive role. We also show that *PTENP1* locus is selectively lost in human cancer. We extend our analysis to other cancer-related genes that possess pseudogenes, such as oncogenic KRAS. Further, we demonstrate that the transcripts of protein coding genes such as *PTEN* are also biologically active. Together, these findings attribute a novel biological role to expressed pseudogenes, as they can regulate coding gene expression, and reveal a non-coding function for mRNAs.

In human cancers, monoallelic mutation of *PTEN* without loss or mutation of the second allele is prevalent at presentation, while complete loss is observed at low frequencies with the exception of advanced cancers[1]. In mouse models, heterozygosity for *Pten* leads to multiple cancers[2], and serial reduction of *Pten* dosage has critical consequences for the incidence and severity of epithelial cancers[3,4], together suggesting that *PTEN* is a functionally haploinsufficient tumour suppressor gene. The identification and validation of

Correspondence and requests for materials should be addressed to P.P.P. (ppandolf@bidmc.harvard.edu).
[†]Present Address: Department of Dermatology, New York University Medical Center, New York, NY 10016, USA
[*]These authors contributed equally to this study.

AUTHOR CONTRIBUTIONS

P.P.P. spearheaded and supervised the project; L.P., L.S. and P.P.P. designed experiments; L.P., L.S. and W.H. performed experiments; B.C. provided prostate cancer patient sample cDNAs. J.Z. performed all bioinformatic analyses. L.P., L.S., and P.P.P. analyzed the data and wrote the paper. All authors critically discussed the results and the manuscript.

numerous *PTEN*-targeting microRNAs demonstrates that post-transcriptional regulation plays a pivotal role in determining PTEN abundance in cancer cells[5–11]. Cells are ultrasensitive to even subtle decreases in PTEN abundance, thus highlighting the importance of microRNA-mediated PTEN regulation in cancer[4]. Therefore, we reasoned that the relationship between PTEN and its pseudogene *PTENP1* (*PTH2*/*ψPTEN*)[12] could represent a compelling test for our hypothesis (Fig. 1a).

Pseudogenes are defined as genomic *loci* that resemble real genes, yet are considered biologically inconsequential because they harbour premature stop codons, deletions/insertions and frameshift mutations that abrogate their translation into functional proteins. Nevertheless, nucleotide sequences contained within pseudogenes are well preserved, suggesting that selective pressure to maintain these genetic elements exists, and that they may indeed play an important cellular role.

Pseudogenes exist as either processed or non-processed genetic elements. While non-processed pseudogenes arose from genetic duplications, processed pseudogenes were generated through retrotransposition; thus they contain no introns yet they commonly share 5’ and 3’ UTR sequences with their ancestral genes[13]. Pseudogenes are almost as numerous as coding genes and represent a significant proportion of the “transcriptome”[14]. Despite lacking canonical promoters, processed pseudogenes utilize proximal regulatory elements to mediate their transcription[15]. Their transcription exhibits tissue-specificity[16] and is aberrantly activated in cancer[17,18], suggesting that pseudogenes may contribute to carcinogenesis, although the mechanisms still remain elusive. Very few pseudogenes have been functionally characterized thus far[13].

MicroRNAs, a large class of small non-coding RNAs (ncRNAs), have emerged as a critical element in cellular biology and pathophysiology. microRNAs have been demonstrated to impact almost all cellular processes and cell types from plants to humans[19]. microRNAs function by annealing to complementary sites on coding sequences or 3’UTRs of target gene transcripts, where they promote the recruitment of protein complexes that impair translation and/or decrease the stability of mRNA leading to a decrease in target protein abundance[19–22]. Physiologically, aberrant expression of microRNAs has been causally linked to human diseases and cancer[23].

We have tested whether pseudogene-derived RNA transcripts and mRNA transcripts possess an active biological role in cancer that is independent of their protein-coding function but would rely upon their ability to compete for microRNA binding, thereby modulating the derepression of microRNA targets (Fig. 1a).

PTENP1 is targeted by *PTEN*-targeting microRNAs

PTENP1 is a processed pseudogene residing at 9p13.3; it is highly homologous to *PTEN*, with only 18 mismatches throughout the coding sequence. A missense mutation of the initiator methionine codon prevents translation[12]. *PTENP1* possesses a 3’-UTR that is ~1kb shorter than that of *PTEN* (Fig. 1b). It can be divided into 2 regions relative to its homology with the *PTEN* 3’UTR: a high homology (~95%) 5’ region and a low homology (<50%) 3’ region (Fig. 1b, Supplementary Fig. 1). Within the high homology region, we found

perfectly conserved seed matches for the *PTEN*-targeting *miR-17*, *miR-21*, *miR-214*, *miR-19* and *miR-26* families (Fig. 1c, Supplementary Fig. 1). To measure the role of these microRNAs on both *PTEN* and *PTENP1* expression, we designed specific PCR primer sets in the non-homologous 3'UTR regions (Supplementary Fig. 2a,b). In DU145 prostate cancer cells, *PTEN*-targeting microRNAs *miR-19b* and *miR-20a* suppress both *PTEN* and *PTENP1* mRNA abundance (Fig. 1d, Supplementary Fig. 3a). In these cells, a pool of inhibitors of endogenously expressed *PTEN*-targeting microRNAs (Supplementary Fig. 3b) de-repressed both *PTEN* and *PTENP1* transcript levels (Fig. 1e). The use of chimeric luciferase plasmids indicated the microRNA:*PTENP1* interaction was direct (Supplementary Fig. 4a–c). These data indicate that *PTENP1* and *PTEN* are subjected to the same microRNA-mediated, post-transcriptional regulation.

The 3'UTR of *PTENP1* has tumour suppressive activity

We examined the ability of *PTENP1* 3'UTR to function as a decoy of *PTEN*-targeting microRNAs using a retroviral vector expressing this 3'UTR (Supplementary Fig. 5a). The 3'UTR can be transcribed, but it cannot code for protein; however it still may exert a biological role. Indeed, *PTENP1* 3'UTR overexpression resulted in a derepression of both PTEN transcript and protein (Fig. 2a, Supplementary Fig. 5b and 10c). Consistent with elevated PTEN, AKT phosphorylation was reduced upon stimulation of cells with EGF (Fig. 2b). These molecular observations were accompanied by growth inhibition (Fig. 2c, Supplementary Fig. 5c and 10d) and a significant reduction in the number of colonies generated in semisolid medium (Fig. 2d).

The derepression of *PTEN* abundance by *PTENP1* 3'UTR overexpression was blunted in HCT116-DICER$^{-/-}$ colon carcinoma cells (Fig. 2e). In these cells, the disruption of DICER -- the enzyme that catalyzes the last step of microRNA maturation -- leads to reduced levels of mature microRNAs compared to parental HCT116 cells[24]. This in turn supports the notion that the 3'UTR of *PTENP1* requires mature microRNAs for its function towards *PTEN*.

To examine the phenotypic consequences of *PTENP1* downregulation, we designed custom siRNA pools (Dharmacon) to specifically target either *PTENP1* (si-PTENP1) or *PTEN* (si-PTEN) expression (Supplementary Fig. 6) since commercially available si-RNA pools for *PTEN* (si-PTEN/PTENP1) bind to common sequences in *PTEN* and *PTENP1* (Supplementary Fig. 7a). si-PTENP1 transfection accelerated cell proliferation, suggesting that *PTENP1*, although expressed at lower relative levels, can exert a biological activity in DU145 cells (Fig. 2f). si-PTEN/PTENP1, which silences both *PTEN* and *PTENP1*, showed the strongest effect, indicating that PTEN and its pseudogene may have additive roles for growth suppression. *PTENP1* knockdown resulted in decreased *PTEN* mRNA and protein abundance (Fig. 2g–h), mirroring the results obtained with overexpression of *PTENP1* 3'UTR (Fig. 2a).

In DU145 cells *PTENP1* 3'UTR is a more potent growth suppressor compared to PTEN (Fig. 2d, Supplementary Fig. 5c). This result may be explained by the fact that microRNAs for which *PTENP1* functions as a decoy also bind other targets with tumour suppressive

activities. For instance, the *miR-17* family targets E2F1 and p21[25], and *miR-21* targets PDCD4[26]. Accordingly, *miR-17* and *miR-21* mimics increase proliferation of *PTEN*-null PC3 cells (Supplementary Fig. 8a), suggesting PTEN independency. Indeed, si-PTENP1 resulted in a dose-dependent downregulation not only of PTEN, but also of p21 (Supplementary Fig. 8b). Additionally, both si-PTENP1 and si-PTEN/PTENP1 were able to suppress *PTENP1* and increase proliferation in a dose-dependent manner in *PTEN*-null PC3 cells (Supplementary Fig. 8c–d). Conversely, stable infection of *PTENP1* 3'UTR in PC3 cells suppressed foci formation (Supplementary Fig. 8e), supporting the notion that *PTENP1* and its 3'UTR exert a tumour suppressive role that goes beyond the regulation of *PTEN* abundance alone.

Expression and losses of *PTENP1* in human cancer

PTEN and *PTENP1* expression was explored in normal human tissues and prostate tumour samples, utilizing custom Taqman probes (see Methods, Supplementary Fig. 2c). In both the normal tissue and prostate tumour arrays, the direct correlation ($r = 0.8087$, $p < 0.0001$ and $r = 0.3960$, $p = 0.0013$, respectively) between *PTEN* and *PTENP1* expression suggests that they may be co-regulated (Fig. 3a–b). This finding supports our molecular observations that *PTENP1* can regulate *PTEN* expression. *PTENP1* was found to be variably abundant, and in some cases expressed at higher levels than *PTEN*.

Next, we examined alterations of the *PTENP1* genomic locus. Several array-based comparative genomic hybridization databases were mined including *The Cancer Workbench* (https://cgwb.nci.nih.gov/cgi-bin/heatmap) and NCBI GEO (http://www.ncbi.nlm.nih.gov/geo/). (Supplementary Fig. 9a–b, Table S1). Remarkably, in a dataset of sporadic colon cancer (http://www.ncbi.nlm.nih.gov/projects/geo/query/acc.cgi?acc=GSE16125) (Fig. 3c–e), hierarchical clustering identified a clear population of samples with detectable copy number (CN) losses occurring specifically at the *PTENP1 locus* (Fig. 3c). Importantly, these CN losses were focal, not associated with large losses of 9p, and independent of losses at the *CDKN2A locus* (Supplementary Fig. 9c). T his data set formally demonstrates the existence of independent genomic CN losses at the *PTENP1 locus*, supporting the notion that *PTENP1* exerts tumour suppressive functions and is under selective pressure to undergo CN losses in cancer.

In the same patient samples set, cluster analysis of *PTEN* expression showed that it was down-regulated compared to normal colon samples ($p = 0.0008156$; Fig. 3d). Regression analysis of *PTENP1* CN variation with the expression levels of *PTEN* identified two discrete populations of patients in which *PTENP1* CN variation and *PTEN* expression were directly and significantly correlated (Population 1: $r = 0.6015$, $p = 0.0092$; Population 2: $r = 0.6056$, $p = 0.0129$) (Fig. 3e). The existence of a direct relationship between *PTENP1* CN and *PTEN* expression supports our hypothesis that *PTENP1* transcript levels can regulate *PTEN* expression. Together, these findings constitute a proof of principle for the oncosuppressive activity of *PTENP1*.

A general model for endogenous mRNA-mediated biology

Based on our results, we expected that the *PTEN* 3'UTR would also have biological activity. Indeed, we found that *PTEN* 3'UTR can derepress *PTENP1* abundance, as *PTENP1* does on *PTEN* (Fig. 4a, left and Supplementary Fig. 10a-c). Importantly, *PTEN* 3'UTR overexpression was accompanied by growth inhibition, suggesting that *PTEN* exerts its tumour suppressive activity, at least in part, through its 3'UTR (Fig. 4a, right and Supplementary Fig. 10d).

To extend our studies beyond *PTEN* and its pseudogene, we examined other cancer-related pseudogenes and genes (Table S2 and S3, Supplementary Fig. 11–17). Alignments of gene and pseudogenes sequences show that microRNA-binding sites are well conserved; for example, the *miR-145* binding site on *OCT4* and its pseudogenes *OCT4-pg1*, *3*, *4* and *5* (Supplementary Fig. 11a); *miR-1* family binding sites on *CONNEXIN 43* (*CX43*) and its pseudogene (Supplementary Fig. 11b). Notably, *OCT4-pg1* and *-pg5* are exclusively expressed in cancer tissues and not in normal tissues[17]. Furthermore *OCT4-pg5* is truncated at the 5' end and expresses only a partial open reading frame region followed by the 3'UTR[27]. Further examples of such conservation include: *miR-34* family binding site on *CDK4PS* (Supplementary Fig. 12); *miR-182* binding site on *FOXO3B* (Supplementary Fig. 13); *miR-17* family binding site on *E2F3P1* (Supplementary Fig. 14); *miR-143* and *let-7* family binding sites on *KRAS1P* (Supplementary Fig. 15).

Since the 3'UTR of *PTENP1* was growth suppressive like its parental gene *PTEN*, we hypothesized a similar relationship between *KRAS* and its pseudogene *KRAS1P*. Indeed, *KRAS1P* 3'UTR overexpression in DU145 cells resulted in increased *KRAS* mRNA abundance (Fig. 4b, left and Supplementary Fig. 18a,b) and accelerated cell growth (Fig. 4b, right). We also found that the *KRAS* and *KRAS1P* transcript levels are positively correlated in prostate cancer (Supplementary Fig. 18c). Notably, the *KRAS1P locus* at 6p11–12, is amplified in different human tumours, including neuroblastoma, retinoblastoma and hepatocellular carcinoma[28–30]. Together these findings point to a putative proto-oncogenic role for *KRAS1P*, and support the notion that pseudogene functions mirror the functions of their cognate genes as explained by a microRNA decoy mechanism.

Discussion

The findings presented in this study have allowed us to reach a number of important conclusions. First, the discovery of a microRNA-decoy function for pseudogenes identifies these transcripts as biologically active units. We show that *PTENP1* and *KRAS1P* affect the levels of their cognate genes and are possibly involved in disease pathogenesis. Thus, the analysis of pseudogene expression level and genomic status in tumourigenesis needs to be undertaken systematically to further our understanding of disease progression.

Processed pseudogenes in mouse oocytes have been previously reported to generate endogenous small interfering RNAs (endo-siRNAs) that downregulate the expression of cognate genes through conventional RNA interference[31]. However, endo-siRNA production has yet to be identified in somatic human cells[32]. Notably, while only few pseudogenes

undergo antisense transcription, all transcribed pseudogenes can in principle compete with cognate genes for microRNA binding. Similarly, the microRNA-decoy capacity of pseudogenes is likely to be more widespread than their cleavage into piRNAs, which have been recently discovered only in germ cells of many organisms, including mouse[33].

We also demonstrate that pseudogenes such as *PTENP1* can derepress their cognate genes, even when expressed at lower levels (Supplementary Fig. 3a and Fig. 2f–h). We propose that pseudogenes are "perfect decoys" for their ancestral genes, because they retain many of the microRNA binding sites and can compete for the binding of many microRNAs at once. It has been hypothesized that suboptimal "pseudotargets" may compete with authentic targets for microRNA binding[34]. By contrast, we propose that pseudogenes have an intrinsic biological activity in microRNA networks because they are legitimate microRNA targets and compete with other legitimate targets for microRNA binding (Fig. 2e). This notion is corroborated by the "target mimicry" process that in plants is achieved by the expression of non-protein coding genes that sequester microRNAs[35].

Exogenously administered microRNA sponges have recently emerged as effective and specific inhibitors of microRNAs[36,37]. Pseudogenes act like "endogenous sponges", able to affect the distribution of microRNA molecules on all their targets. They may be particularly effective precisely because they are non-coding, thus active translation does not interfere with microRNA binding[38].

The ability of pseudogenes to regulate the biology of a cell goes beyond their ability to modulate the levels of their cognate gene (Supplementary Fig. 8). This phenomenon is consistent with the fact that each microRNA has multiple targets and can lead to widespread homeostatic effects. Also, given that a single gene often has numerous differentially regulated pseudogenes (*e.g. OCT4*, *NPM1* (Supplementary Figs. 11a, 17) and ribosomal protein pseudogenes[39]), such networks can become intricately dynamic.

Cellular microRNA abundance is dictated by total genomic CN and by their biogenesis process[40]. Less is known about the regulation of mature microRNA activity. microRNAs can increase their spectrum of targetable mRNAs by undergoing deamination[41], while shortening of 3'UTRs[42] and polymorphisms can prevent microRNA binding to mRNAs[43]. Pseudogene-mediated microRNA decoys offer a new dimension regulating the cross-talk between microRNAs and their targets. Indeed the greater the number of pseudogenes that a protein-coding gene has, the more it is protected from microRNAs.

Our discovery of a functional role for *PTENP1* is relevant to PTEN biology since minute changes in PTEN can have tumourigenic consequences[3]. In our analysis we found that *PTENP1* positively regulates *PTEN* levels. Furthermore, we found that the *PTENP1 locus* undergoes CN losses in human cancer and this correlates with decrease in *PTEN*; thus we propose that *PTENP1* is a *bona fide* tumour suppressor gene. In light of this, better tools must be developed to detect pseudogene abundance in cancer. For instance, pseudogenes including *PTENP1* have been overlooked to such an extent that pseudogene-specific probes are absent in some microarray platforms (Supplementary Figure 7b).

An important implication of our findings is that the decoy mechanism may not be limited to pseudogenes, but may include other long ncRNA transcripts including ribosomal RNAs, lincRNAs and coding gene mRNAs[39,44] (Fig. 4a and Supplementary Fig. 10). Beyond their function as *cis* regulatory elements that impact the stability of their own transcripts, UTRs are also *trans* modulators of gene expression through microRNA binding. Furthermore, since binding sites for microRNAs are also located in open reading frame sequences[21], the entire transcript of coding genes, and not only the 3'UTR may possess decoy function (see working model: Fig. 4c).

As our model suggests, mRNA introduced into a cell can potentially perturb the interaction between microRNAs and their multiple targets and thus, have a biological activity independent of the translation of the protein they encode[45]. Importantly, the same applies to the transcriptional induction or repression of endogenous mRNA levels, which can lead to changes in the number of mRNA molecules present within a cell in the scale of several orders of magnitude[46].

Our findings indicate that, when studying specific nonsense or frameshift mutations and genomic alterations leading to "readthrough" or fusion transcripts, one must consider this new RNA-regulated biological dimension. For example, chromosomal fusion events such as the t(15;17) translocation of APL which generates *PML-RARα* and *RARα-PML* fusion transcripts or recurrent "readthrough" transcripts in melanoma such as *CDK2-RAB5B* could exert oncogenic activities through an aberrant microRNA "sponging" activity[47,48]. This phenomenon could also occur as a consequence of somatic genomic rearrangements, which are emerging as grossly unappreciated events in many cancers[49]. Moreover, the shortening of 3'UTRs as observed in human cancer cells[42] would not solely affect microRNA-dependent mRNA regulation, but on the flipside, also alter the "sponging" capacity of a given RNA transcript. Finally, in the case of *PTEN*-loss associated cancers, there is little known of the molecular consequences of PTEN mutations where the *PTEN* transcript is retained, compared to complete genetic loss of *PTEN* where no transcript remains[1]. While these events were previously thought to alter protein abundance, protein signaling and protein networks, they will also have a significant impact on cellular RNA and microRNA homeostasis. In this study, we have therefore identified a novel dimension by which cellular and tumour biology can be regulated.

Methods Summary

Cell lines were cultured under standard conditions. microRNA overexpression was measured by transient transfection (si-miRNAs). *PTENP1*/*PTEN*/*KRAS1P* 3'UTR overexpression was achieved by transient transfection (**pCMV** expression vectors) or stable infection with **MSCV-PIG** retroviral constructs. miRNA/target interaction was measured by a luciferase reporter assay. *PTENP1*, *PTEN*, *KRAS*, *KRAS1P* and miRNA expression level was detected by real time PCR. Proliferation, foci and soft agar assay were performed according standard protocols.

METHODS

Reagents

Anti-HSP90 antibody #61041 (Becton Dickinson); anti-PTEN antibody #9559, antip21 antibody #2947, anti-Tubulin antibody #2125; siGENOME non-targeting siRNA #2 (siLuc), si-PTEN, si-PTENP1, si-PTEN/PTENP1, siGLO RISC-free control siRNA, si-miR-17, si-miR-19b, si-miR20a, si-miR-21, si-miR-26b, si-miR-214, microRNA inhibitor negative control #1 (IC), miR-19b inhibitor, miR-93 inhibitor, miR-106b inhibitor, Dharmafect 1 (Dharmacon); lipofectamine 2000, Trizol Reagent, DNAseI amplification grade, SuperScript II reverse transcriptase, Dulbecco's Modified Eagle Medium (D-MEM), RPMI-1640, foetal bovine serum (FBS) (Invitrogen); Tissue Scan Normal Tissue qPCR Arrays: Human Major Tissue (HMRT103); Tissue Scan Disease Tissue qPCR Arrays: Prostate Cancer II (HPRT102) (Origen); pGL3-Control, pRL-TK, Dual-Luciferase reporter assay (Promega); polybrene, puromycin (Sigma); QuantiTect Sybr Green PCR kit, Effectene (Qiagen); EGF (R&D); QuikChange II XL Site-Directed Mutagenesis Kit, Herculase Taq polymerase (Stratagene).

Plasmids

The 3'UTR of *PTENP1* (NM_023917) was amplified by PCR from the genomic DNA of PC3 cells and cloned into the BamHI and XhoI sites of pCMV-MCS expression plasmid. In this way, pCMV/ψ3'UTR plasmid was obtained. The primers used for PCR amplification were: F 5'-GAGGAGCCGTCAAATCCAGAG-3' and R 5'-TCGTCAATGTGTGAGGTTCC-3'. The 3'UTR of *PTENP1* was then subcloned into the BglII and XhoI sites of MSCV-PIG retroviral vector[50] to obtain PIG/ψ3'UTR plasmid. The 3'UTR of *PTEN* (NM_000314.4) was amplified by PCR from the genomic DNA of HeLa cells and cloned into the BamHI and XhoI sites of pCMV-MCS expression plasmid. In this way, pCMV/PTEN3'UTR plasmid was obtained. The primers used for PCR amplification were: F 5 '-TAGAGGAGCCGTCAAATCCA-3 ' and R 5'-TGGACATCTGATTGGGATGA-3'. The 3'UTR of *KRAS1P* (NC_000006.11) was amplified by PCR from the genomic DNA of HeLa cells and cloned into the BamHI and XhoI sites of pCMV-MCS expression plasmid. In this way, pCMV/K1P3'UTR plasmid was obtained. The primers used for PCR amplification were : F 5 '-AACCAGCAAAGACAGGGTGT-3' and R 5'-GTTCAATTGCTCAACGCAGA-3'. The homology between wt *KRAS* and its pseudogene is very high (> 90%) across the whole mRNA sequence. The primers used for the amplification of *KRAS1P* 3'UTR contain many mismatches which made them specific for the pseudogene. In order to construct pGLU/ψ3'UTR chimeric luciferase plasmid, the multicloning site of pGL3-Control plasmid was removed from its original position and inserted into the XbaI site located downstream of Luciferase STOP codon (pGLU). *PTENP1* 3'UTR was then subcloned from pCMV/ψ3'UTR plasmids using the SmaI and XhoI sites of pGLU. The QuikChange II XL Site-Directed Mutagenesis Kit was used to generate the mutated version of this plasmid (pGLU/ψ3'UTRmut).

Cells and culture conditions

Phoenix A, 293T and PC3 cells were grown in DMEM +10% FBS. RWPE-1, PWR-1E and VCaP were grown in keratinocyte medium + EGF + BPE. 22Rv1, DU145[51] and LnCaP were grown in RPMI 1640 + 10% FBS. All cell lines were obtained from ATCC and grown in penicillin/streptomycin and glutamine containing medium, at 37°C in a humidified atmosphere with 6% CO_2.

Transient transfection

For the transfection of si-miRNAs / microRNA inhibitors, DU145 (1.5×10^5) or PC3 (1×10^5) were seeded in 12-well dishes. The following day they were transfected with 100nM siRNAs/si-microRNAs or 400nM microRNA inhibitors using Dharmafect 1 according to the manufacturer's recommendations. With this protocol more than 90% of cells were positive to the fluorescent siGLO RISC-free control siRNA (data not shown). The day after the transfection cells were trypsinized and reseeded in 12 well plates for subsequent collection and analysis.

For plasmid transfection, 293T and DU145 were seeded in 6cm dishes (2.5 and 3.5×10^5, respectively) and the day after they were transfected with Effectene. 6h later, they were trypsinized and seeded for the various assays.

Dual luciferase reporter assay

DU145 cells were seeded at a density of 6×10^4 cells per 24-well dish. 24 hours later, 720 ng of pGLU/ψ3'UTR or pGLU/ψ3'UTRmut were cotransfected with 80 ng of pRL-TK. Lipofectamine 2000 was used as transfectant. 24h after transfection, luciferase activity was measured and normalized as in Ref. [7].

Retroviral infection

Phoenix A cells were plated in 10cm poly-D-Lysine coated dishes (3×10^6/dish) and, 16 hours later, were transfected with PIG retroviral plasmids using Lipofectamine 2000. 48 hours later, the virus-containing medium (10 ml) was filtered, mixed with 5 ml of freshly prepared medium, supplemented with 4 μg/ml polybrene and added to 5×10^5 DU145 or PC3 cells plated in a 10 cm dish the day before. Puromycin (2 μg/ml) was administered 48 hours after infection. The cells were selected for 2 days and then utilized for the various assays. Selection medium was changed everyday.

PCR analysis

Total RNA was extracted using Trizol reagent according to the manufacturer's instructions. It was then subjected to DNase treatment and retrotranscription (1 μg RNA/vial).

Regular PCR was performed using Herculase Taq Polymerase.

Real time PCR of *wt PTEN*, *PTENP1*, *KRAS* and *KRAS1P* was carried out using Sybr Green fluorescence. 2 μl of RT were used in a 20 μl reaction. *ACTIN* was used as an internal standard. Relative quantification of gene expression was performed with the comparative C_T method[52]. *PTEN* primers: F 5'-GTTTACCGGCAGCATCAAAT-3'; R 5'-

CCCCCACTTTAGTGCACAGT-3'. *PTENP1* primers: F 5'-TCAGAACATGGCATACACCAA-3'; R 5'-TGATGACGTCCGATTTTTCA-3'. *KRAS* primers: F 5'-ATTGTGAATGTTGGTGT-3 ' ; R 5 '-GAAGGTCTCAACTGAAATT-3'. *KRAS1P* primers: F 5'-AAGGTTTCTTCCAGTTCT-3 ' ; R 5 '-ATTTGGGAATTTTGTGAG-3'. *ACTIN* primers: F 5'-CATGTACGTTGCTATCCAGGC-3'; R 5'-CTCCTTAATGTCACGCACGAT-3'.

The real time PCR of mature microRNAs was performed according to Ref. 53 with some modifications. Briefly, an independent retrotranscription reaction was set up for each microRNA using 0.05μM of the microRNA-specific RT primer and 0.05μM of SNORD44 RT primer (5'-GTCGTATCCAGTGCAGGGTCCGAGGTATTCGCACTGGATACGACagtcag-3 '). Real-time PCR of both the microRNA and SNORD44, which was used as an internal standard, were then carried out using Sybr Green fluorescence (2 μl of RT in a 20 μl reaction). For the microRNA, a specific forward primer and the universal R primer (5'-GTGCAGGGTCCGAGGT-3') were used. For SNORD44, 5'-CGGCGGtggcgatgaggaggtacc-3' forward primer and the universal reverse primer were used. The microRNA-specific RT and forward PCR primers are listed in Supplementary Fig. 19. The Real-time PCR reaction comprised 40 cycles of 95°C for 15sec followed by 60°C for 1min. Relative quantification of gene expression was performed with the comparative C_T method as described above.

TaqMan RT PCR was performed at the HMS Biopolymers Facility utilizing an Applied Biosystems 7900 HT Fast instrument.

Western blot

Cells were collected and lysed (50mM Tris pH8.0, 1mM EDTA, 1mM $MgCl_2$, 150mM NaCl, 1% NP-40, 1 mM β-glycerophosphate, 1 mM Na_3VO_4, 1 mM NaF, protease inhibitors). Proteins (30 μg/lane) were separated on 10% SDS-polyacrylamide gel and transferred to nitrocellulose membrane. Immunoblotting of the membranes was performed using the following primary antibodies: anti-PTEN (1:1000), anti-p21 (1:1000), anti-HSP90 (1:1000), anti-Tubulin (1:2000). Signals were revealed after incubation with recommended secondary antibody coupled to peroxidase by using enhanced chemiluminescence. Scanned images were quantified using ImageJ software.

FACS analysis

After 10 min treatment with 50 ng/ml EGF, cells were scraped from 10 cm dishes, immediately fixed in 4%PFA and permeabilized with ice cold Methanol. After rehydrating with 0.1%BSA in PBS, cells were stained with Phospho-Akt (Thr308) Rabbit mAb -Alexa Fluor® 647 Conjugate (Cell Signaling). Cells were analyzed on an LSRII flow cytometer (BD).

Cell proliferation

At the end of the selection period (infection) or 6h post-transfection, 2×10^5 DU145 cells were trypsinized, resuspended in 50ml and seeded in 8 sets of 3 wells of a 12-well plate.

Starting from the following day (d0), 1 set of wells per day was washed once with PBS, fixed in 10% formalin solution for 10min at room temperature and then kept in PBS at 4°C. At day 7, all the wells were stained with crystal violet. After lysis with acetic acid 10%, O.D. was read at 590 nm.

Foci assay

At the end of the selection period (infection) or 6h post-transfection, DU145 or PC3 cells were trypsinized. 5×10^3 cells were plated on 10cm dishes. 14–21 days later, the plates were stained with crystal violet and the foci were counted.

Growth in semisolid medium

The bottom layer was obtained by covering 6-well dishes with 3 ml of 0,6% agar in DMEM. The day after, 5×10^4 infected cells were seeded on top in triplicate in 2 ml of 0,3% agar in DMEM + 10%FBS. Colonies were counted after 3–4 weeks at 40× magnification.

Analysis of *PTEN* and *PTENP1* genomic status and expression

Breast Cancer: Affymetrix GeneChip® Human Mapping 500K Array datasets GSE7545 and GSE16619 were downloaded from NCBI GEO and analyzed with the Partek Genomic Suite (Partek Inc) for detection of genomic regions with alterations and data visualization. Copy number aberrations were scored with the Partek segmentation algorithm with default paramaters: p-value cutoff at 0.001 for neighboring regions with significantly different means, 10 minimum number of probe sets required for any candidate region, 0.3 signal to noise difference as minimum magnitude of change, and p-value threshold 0.01 for one-sided t-test of probes in each region to be considered as significantly deviated from the expected normal. All aberrations were calculated with respect to a set of 270 HapMap-normal persons. 118 breast cancer samples and 44 normal samples were included in the study.

Colon Cancer: GSE16125 sporadic colon cancer raw datasets were downloaded from NCBI GEO (http://www.ncbi.nlm.nih.gov/projects/geo/query/acc.cgi?acc=GSE16125). There are two chip platforms employed in this dataset: 48 sporadic colon cancer samples interrogated by Affymetrix GeneChip(r) Human Mapping 250K Nsp SNP Array and 36 of them analyzed by Affymetrix Human Exon 1.0 ST Array. The SNP array raw datasets were analyzed with the Partek Genomic Suite (Partek Inc) for detection of genomic regions with alterations and data visualization (Partek smoothing algorithm was based on 46 probes). Fortyeight normal samples from the HapMap project supplied by Affymetrix were used as an un-paired reference set [http://www.affymetrix.com/support/technical/sample_data/500k_data.affx]. Raw exon array intensity CEL files for colon cancer and normal colon were analyzed by Affymetrix Power Tools (APT, v. 1.12.0). Normalized intensity value for *PTEN* was calculated as average of 8 probes corresponding to two *PTEN* specific exon probe set "3256703" and "3256704". These values were extracted out by APT software. Affymetrix Human Exon 1.0 ST Array dataset for normal colon epithelial cells was downloaded from NCBI GEO GSE1916 dataset (http://www.ncbi.nlm.nih.gov/geo/query/acc.cgi?acc=GSE19163). The correlation plot with r and p values between log10 *PTEN* expression intensity and log-ratio of *PTENP1* copy number was generated in GraphPad Prism

(GraphPad Software, Inc.). The log-ratio of *PTENP1* was based on average of 14 SNP probes flanking *PTENP1* gene.

Statistical analysis

In vitro data were analyzed using unpaired *t*-test (GraphPad Prism, GraphPad Software, Inc.) Values of $p < 0.05$ were considered statistically significant. *$p < 0.05$; **$p < 0.01$; ***$p < 0.001$. The mean ± s.d. of three or more independent experiments is reported. Regression analyses and correlation coefficients were generated using GraphPad Prism, GraphPad Software, Inc.

Supplementary Material

Refer to Web version on PubMed Central for supplementary material.

ACKNOWLEDGMENTS

We thank Pandolfi lab members for critical discussions, in particular A. Carracedo for critical input; S. Feng for technical assistance. We thank Bert VogeIstein for DICER$^{-/-}$ cells; T. Yuan for assistance with FACS analysis; A. Tuccoli for assistance with microRNA RT-PCR; I. Osman for support and insightful suggestions. L.P. was supported by fellowships from the Istituto Toscano Tumori and the American Italian Cancer Foundation. L.S. was supported by fellowships from the Human Frontier Science Program and the Canadian Institutes of Health Research. This work was supported by NIH grant R01 CA-82328-09 to P.P.P.

References

1. Salmena L, Carracedo A, Pandolfi PP. Tenets of PTEN tumor suppression. Cell. 2008; 133:403–414. [PubMed: 18455982]
2. Di Cristofano A, et al. Impaired Fas response and autoimmunity in Pten+/− mice. Science. 1999; 285:2122–2125. [PubMed: 10497129]
3. Trotman LC, et al. Pten dose dictates cancer progression in the prostate. PLoS Biol. 2003; 1:E59. [PubMed: 14691534]
4. Alimonti A, et al. Subtle variations in Pten dose determine cancer susceptibility. Nat Genet. 2010
5. Xiao C, et al. Lymphoproliferative disease and autoimmunity in mice with increased miR-17-92 expression in lymphocytes. Nat Immunol. 2008; 9:405–414. [PubMed: 18327259]
6. Takakura S, et al. Oncogenic role of miR-17-92 cluster in anaplastic thyroid cancer cells. Cancer Sci. 2008; 99:1147–1154. [PubMed: 18429962]
7. Lewis BP, Shih IH, Jones-Rhoades MW, Bartel DP, Burge CB. Prediction of mammalian microRNA targets. Cell. 2003; 115:787–798. [PubMed: 14697198]
8. Meng F, et al. Involvement of human micro-RNA in growth and response to chemotherapy in human cholangiocarcinoma cell lines. Gastroenterology. 2006; 130:2113–2129. [PubMed: 16762633]
9. Huse JT, et al. The PTEN-regulating microRNA miR-26a is amplified in high-grade glioma and facilitates gliomagenesis in vivo. Genes Dev. 2009; 23:1327–1337. [PubMed: 19487573]
10. Kato M, et al. TGF-beta activates Akt kinase through a microRNA-dependent amplifying circuit targeting PTEN. Nat Cell Biol. 2009
11. Yang H, et al. MicroRNA expression profiling in human ovarian cancer: miR-214 induces cell survival and cisplatin resistance by targeting PTEN. Cancer Res. 2008; 68:425–433. [PubMed: 18199536]
12. Fujii GH, Morimoto AM, Berson AE, Bolen JB. Transcriptional analysis of the PTEN/MMAC1 pseudogene, psiPTEN. Oncogene. 1999; 18:1765–1769. [PubMed: 10208437]
13. D'Errico I, Gadaleta G, Saccone C. Pseudogenes in metazoa: origin and features. Brief Funct Genomic Proteomic. 2004; 3:157–167. [PubMed: 15355597]

14. Harrison PM, Zheng D, Zhang Z, Carriero N, Gerstein M. Transcribed processed pseudogenes in the human genome: an intermediate form of expressed retrosequence lacking protein-coding ability. Nucleic Acids Res. 2005; 33:2374–2383. [PubMed: 15860774]
15. Birney E, et al. Identification and analysis of functional elements in 1% of the human genome by the ENCODE pilot project. Nature. 2007; 447:799–816. [PubMed: 17571346]
16. Bristow J, Gitelman SE, Tee MK, Staels B, Miller WL. Abundant adrenal-specific transcription of the human P450c21A "pseudogene". J Biol Chem. 1993; 268:12919–12924. [PubMed: 7685353]
17. Suo G, et al. Oct4 pseudogenes are transcribed in cancers. Biochem Biophys Res Commun. 2005; 337:1047–1051. [PubMed: 16229821]
18. Zhang L, et al. microRNAs exhibit high frequency genomic alterations in human cancer. Proc Natl Acad Sci U S A. 2006; 103:9136–9141. [PubMed: 16754881]
19. Bartel DP. MicroRNAs: target recognition and regulatory functions. Cell. 2009; 136:215–233. [PubMed: 19167326]
20. Baek D, et al. The impact of microRNAs on protein output. Nature. 2008; 455:64–71. [PubMed: 18668037]
21. Tay Y, Zhang J, Thomson AM, Lim B, Rigoutsos I. MicroRNAs to Nanog, Oct4 and Sox2 coding regions modulate embryonic stem cell differentiation. Nature. 2008; 455:1124–1128. [PubMed: 18806776]
22. Lal A, et al. miR-24 Inhibits cell proliferation by targeting E2F2, MYC, and other cell-cycle genes via binding to "seedless" 3'UTR microRNA recognition elements. Mol Cell. 2009; 35:610–625. [PubMed: 19748357]
23. Ventura A, Jacks T. MicroRNAs and cancer: short RNAs go a long way. Cell. 2009; 136:586–591. [PubMed: 19239879]
24. Cummins JM, et al. The colorectal microRNAome. Proc Natl Acad Sci U S A. 2006; 103:3687–3692. [PubMed: 16505370]
25. Petrocca F, et al. E2F1-regulated microRNAs impair TGFbeta-dependent cell-cycle arrest and apoptosis in gastric cancer. Cancer Cell. 2008; 13:272–286. [PubMed: 18328430]
26. Lu Z, et al. MicroRNA-21 promotes cell transformation by targeting the programmed cell death 4 gene. Oncogene. 2008; 27:4373–4379. [PubMed: 18372920]
27. Pain D, Chirn GW, Strassel C, Kemp DM. Multiple retropseudogenes from pluripotent cell-specific gene expression indicates a potential signature for novel gene identification. J Biol Chem. 2005; 280:6265–6268. [PubMed: 15640145]
28. van der Wal JE, et al. Comparative genomic hybridisation divides retinoblastomas into a high and a low level chromosomal instability group. J Clin Pathol. 2003; 56:26–30. [PubMed: 12499428]
29. Zimonjic DB, Keck CL, Thorgeirsson SS, Popescu NC. Novel recurrent genetic imbalances in human hepatocellular carcinoma cell lines identified by comparative genomic hybridization. Hepatology. 1999; 29:1208–1214. [PubMed: 10094966]
30. Plantaz D, et al. Gain of chromosome 17 is the most frequent abnormality detected in neuroblastoma by comparative genomic hybridization. Am J Pathol. 1997; 150:81–89. [PubMed: 9006325]
31. Tam OH, et al. Pseudogene-derived small interfering RNAs regulate gene expression in mouse oocytes. Nature. 2008; 453:534–538. [PubMed: 18404147]
32. Okamura K, Chung WJ, Lai EC. The long and short of inverted repeat genes in animals: microRNAs, mirtrons and hairpin RNAs. Cell Cycle. 2008; 7:2840–2845. [PubMed: 18769156]
33. Robine N, et al. A broadly conserved pathway generates 3'UTR-directed primary piRNAs. Curr Biol. 2009; 19:2066–2076. [PubMed: 20022248]
34. Seitz H. Redefining microRNA targets. Curr Biol. 2009; 19:870–873. [PubMed: 19375315]
35. Franco-Zorrilla JM, et al. Target mimicry provides a new mechanism for regulation of microRNA activity. Nat Genet. 2007; 39:1033–1037. [PubMed: 17643101]
36. Ebert MS, Neilson JR, Sharp PA. MicroRNA sponges: competitive inhibitors of small RNAs in mammalian cells. Nat Methods. 2007; 4:721–726. [PubMed: 17694064]
37. Lee DY, et al. A 3'-untranslated region (3'UTR) induces organ adhesion by regulating miR-199a* functions. PLoS One. 2009; 4:e4527. [PubMed: 19223980]

38. Gu S, Jin L, Zhang F, Sarnow P, Kay MA. Biological basis for restriction of microRNA targets to the 3' untranslated region in mammalian mRNAs. Nat Struct Mol Biol. 2009; 16:144–150. [PubMed: 19182800]
39. Balasubramanian S, et al. Comparative analysis of processed ribosomal protein pseudogenes in four mammalian genomes. Genome Biol. 2009; 10:R2. [PubMed: 19123937]
40. Winter J, Jung S, Keller S, Gregory RI, Diederichs S. Many roads to maturity: microRNA biogenesis pathways and their regulation. Nat Cell Biol. 2009; 11:228–234. [PubMed: 19255566]
41. Kawahara Y, et al. Redirection of silencing targets by adenosine-to-inosine editing of miRNAs. Science. 2007; 315:1137–1140. [PubMed: 17322061]
42. Mayr C, Bartel DP. Widespread shortening of 3'UTRs by alternative cleavage and polyadenylation activates oncogenes in cancer cells. Cell. 2009; 138:673–684. [PubMed: 19703394]
43. Kim J, Bartel DP. Allelic imbalance sequencing reveals that single-nucleotide polymorphisms frequently alter microRNA-directed repression. Nat Biotechnol. 2009; 27:472–477. [PubMed: 19396161]
44. Guttman M, et al. Chromatin signature reveals over a thousand highly conserved large non-coding RNAs in mammals. Nature. 2009; 458:223–227. [PubMed: 19182780]
45. Frith MC, et al. Pseudo-messenger RNA: phantoms of the transcriptome. PLoS Genet. 2006; 2:e23. [PubMed: 16683022]
46. Jiang SL, Lozanski G, Samols D, Kushner I. Induction of human serum amyloid A in Hep 3B cells by IL-6 and IL-1 beta involves both transcriptional and post-transcriptional mechanisms. J Immunol. 1995; 154:825–831. [PubMed: 7814886]
47. Scaglioni PP, Pandolfi PP. The theory of APL revisited. Curr Top Microbiol Immunol. 2007; 313:85–100. [PubMed: 17217040]
48. Berger MF, et al. Integrative analysis of the melanoma transcriptome. Genome Res. 2010; 20:413–427. [PubMed: 20179022]
49. Stephens PJ, et al. Complex landscapes of somatic rearrangement in human breast cancer genomes. Nature. 2009; 462:1005–1010. [PubMed: 20033038]

Methods References

50. Maeda T, et al. Role of the proto-oncogene Pokemon in cellular transformation and ARF repression. Nature. 2005; 433(7023):278–285. [PubMed: 15662416]
51. Myers MP, et al. P-TEN, the tumour suppressor from human chromosome 10q23, is a dual-specificity phosphatase. Proc Natl Acad Sci U S A. 1997; 94(17):9052–9057. [PubMed: 9256433]
52. Drabkin HA, et al. Quantitative HOX expression in chromosomally defined subsets of acute myelogenous leukemia. Leukemia. 2002; 16(2):186–195. [PubMed: 11840284]
53. Chen C, et al. Real-time quantification of microRNAs by stem-loop RT-PCR. Nucleic Acids Res. 2005; 33(20):e179. [PubMed: 16314309]

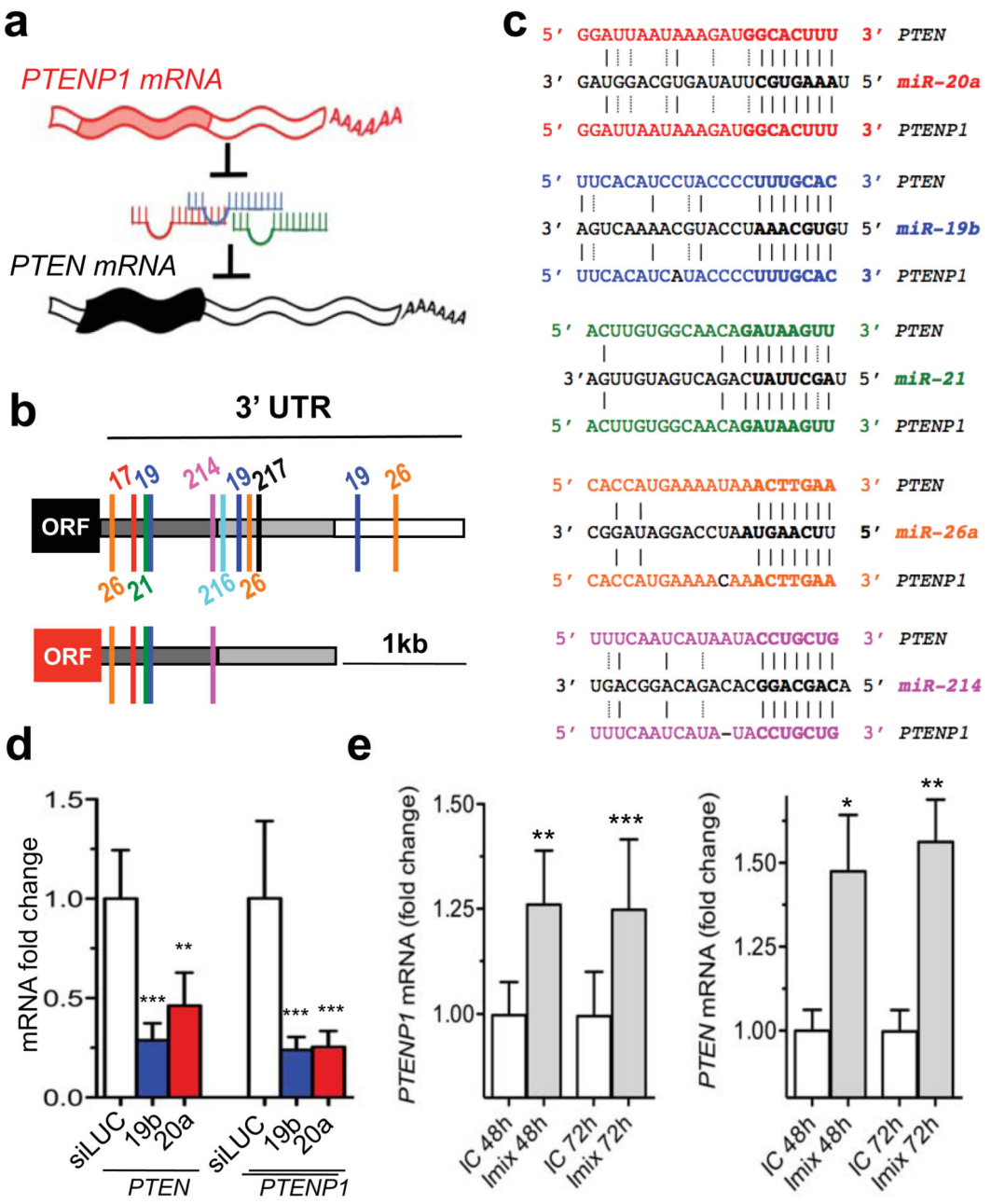

Figure 1. *PTENP1* is targeted by *PTEN*-targeting microRNAs

a. Working hypothesis: *PTEN* is protected from microRNA binding by *PTENP1*. microRNAs: colored squiggles; 5'and 3'UTRs: open rectangles; open reading frames: filled rectangles. **b.** *PTEN* (*upper*) and *PTENP1* (*lower*) 3'UTRs contain a highly conserved (dark grey) followed by a poorly conserved (light grey) domain. *PTEN*-targeting microRNA seed matches within in the high homology region are conserved between *PTEN* and *PTENP1*. **c.** Binding of *PTEN*-targeting microRNAs to *PTENP1*. Seeds and seed matches: bold; canonical pairings: solid lines; non-canonical pairings (G:U): dotted lines. **d.** *PTEN*-

targeting *miR-19b* and *miR20a* decrease *PTEN* and *PTENP1* mRNA abundance. **e.** *miR-17* and *miR-19* family inhibitors derepress *PTENP1* abundance *(left)*. *PTEN* is used as positive control *(right)*. **d** and **e**. mean ± s.d., n ≥ 3.

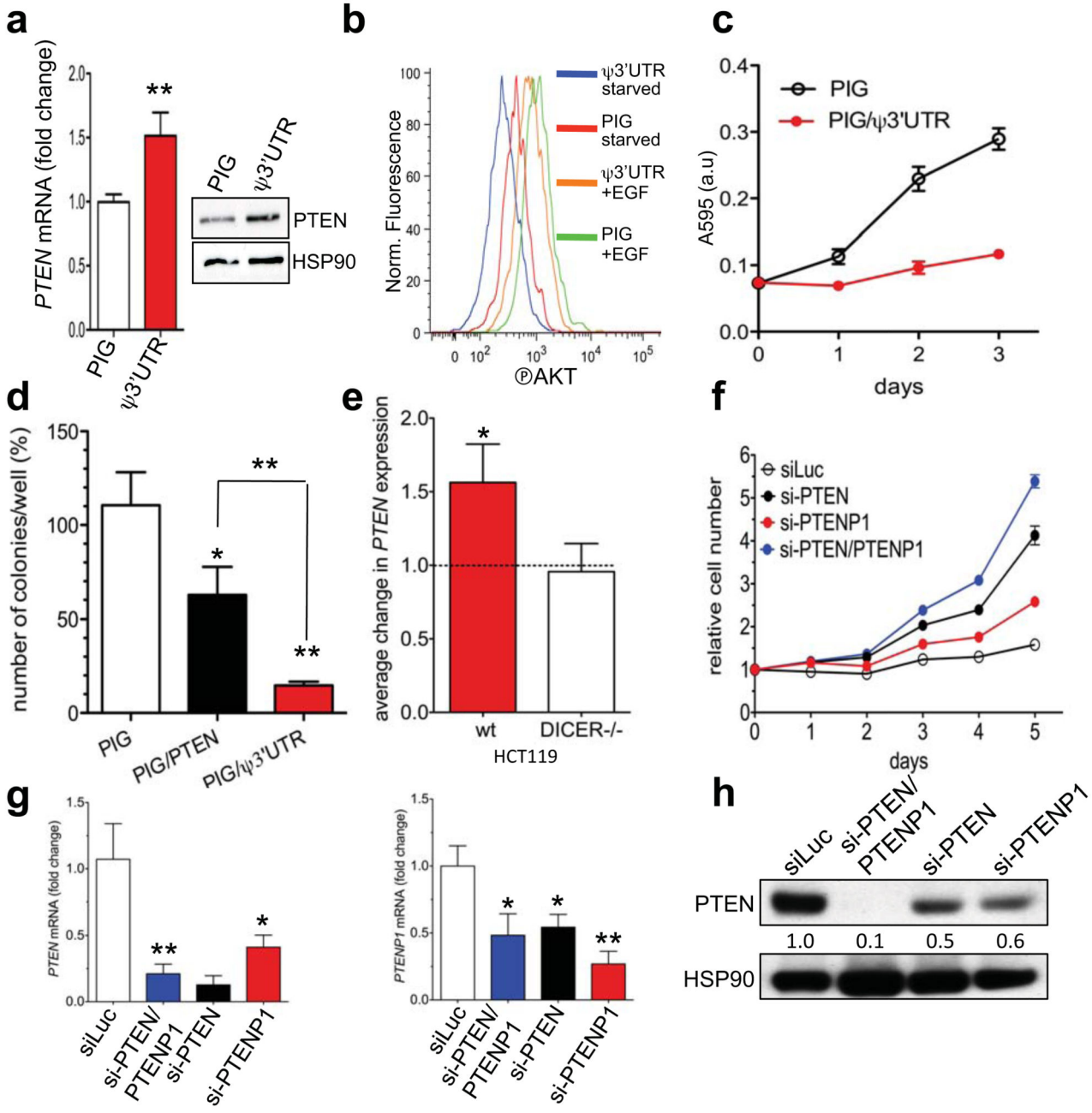

Figure 2. *PTENP1* 3'UTR exerts a tumour suppressive function by acting as a decoy for *PTEN*-targeting microRNAs

a–c. PIG/ψ3'UTR-infected DU145 cells show (**a**) increased *PTEN* mRNA and protein levels (**b**) reduced phosho-AKT levels upon EGF stimulation and (**c**) decreased proliferation rate. **d.** Growth in semisolid medium of DU145 cells infected with **PIG**, **PIG/ψ3'UTR** or **PIG/PTEN**. **e.** *PTEN* mRNA levels 24h after the transfection of **pCMV/ψ3'UTR** in parental HCT116 or HCT116-DICER−/− cells. Data are normalized using **pCMV** empty-transfected cells. **f.** Growth curve of DU145 cells transfected with control siLuc, si-PTEN/

PTENP1, si-PTEN or si-PTENP1. **g.** mRNA levels of *PTEN* (*left*) and *PTENP1* (*right*) 24h after the transfection of siLuc (white), si-PTEN/PTENP1 (blue), si-PTEN (black), si-PTENP1 (red). **i.** Western blot of PTEN 48h after the transfection of the indicated siRNAs. **a**, **c, d**, **e**, **f** and **g.** mean ± s.d., n ≥ 3.

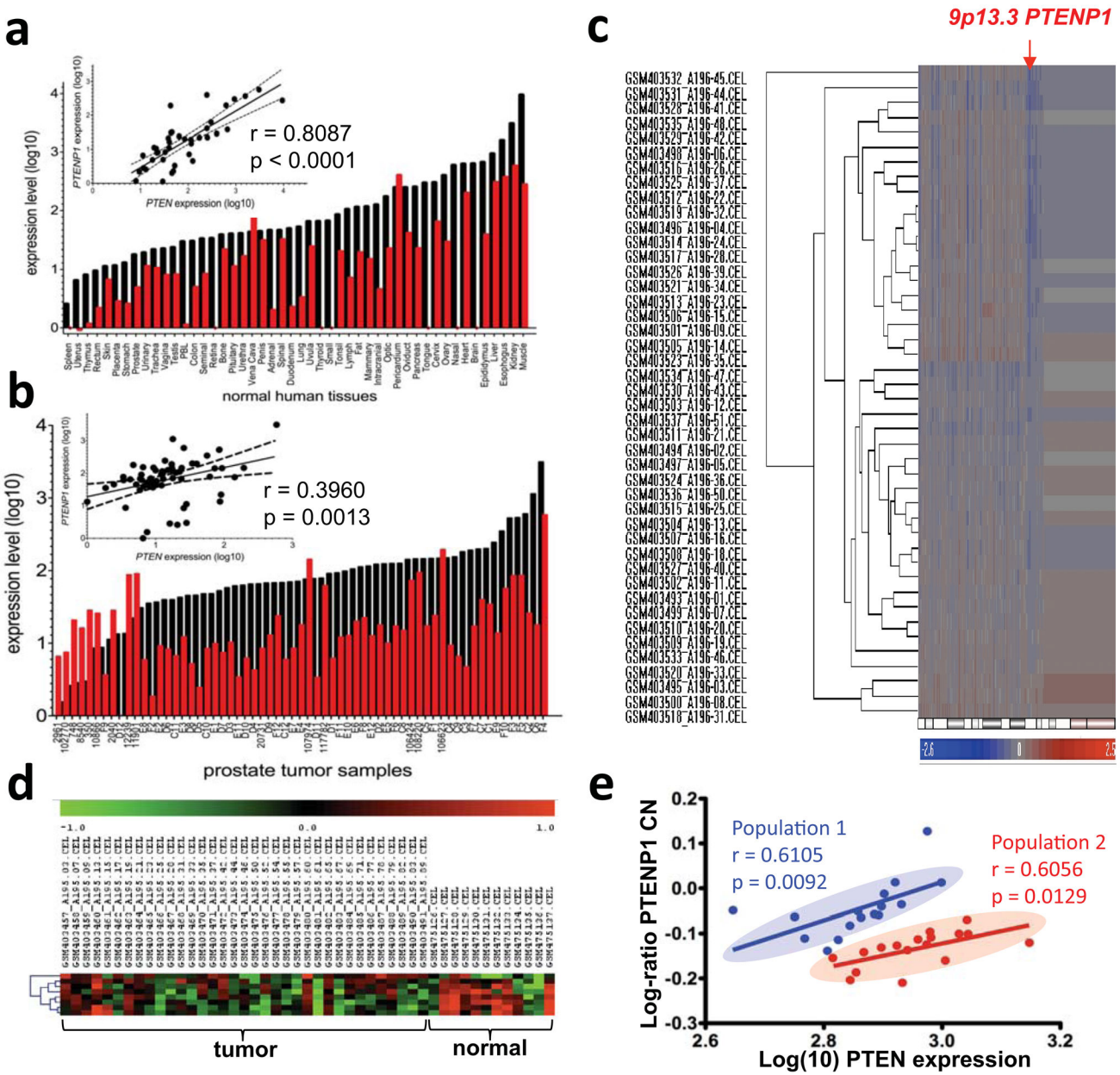

Figure 3. Loss of *PTENP1* in cancer

a–b. Expression level of *PTEN* (*black*) and *PTENP1* (*red*) in a panel of normal human tissues (**a**) and prostate tumour samples (**b**). Linear regression of *PTEN* vs *PTENP1* expression is shown in the upper left corner. **c.** Cluster analysis of 48 sporadic colon cancer samples interrogated by Affymetrix Human SNP Array. **d.** Heat map and Cluster analysis of Affymetrix Human Exon 1.0 ST Array for normalized *PTEN* intensity values. **e.** Plot of log-ratio of *PTENP1* copy number (CN) against log10 *PTEN* expression intensity. Lines of best fit represent regression analyses of two populations. The correlation coefficient (r) measures the reliability and the p-value measures the statistical significance of the correlation between the x and y.

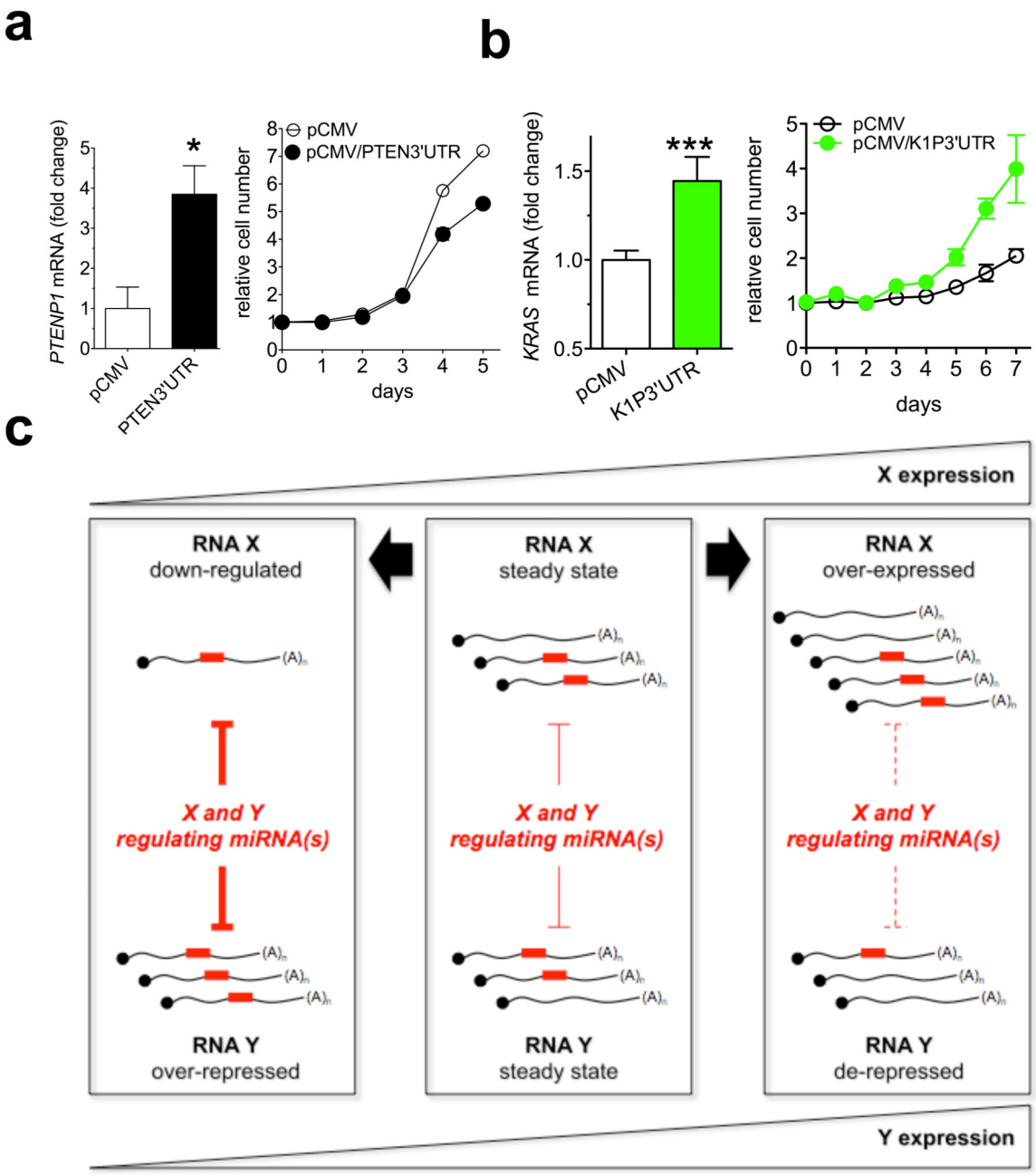

Figure 4. ***PTEN*** **3'UTR and** ***KRAS1P*** **3'UTR function as decoys and a general model for endogenous microRNA decoy mechanism**

a. *PTENP1* mRNA level 24h after the transfection of the empty **pCMV** or **pCMV/PTEN3'UTR** plasmid in DU145 cells (*left*) and growth curve (*right*). **b.** *KRAS* mRNA level 24h after the transfection of the empty **pCMV** or **pCMV/K1P3'UTR** plasmid in DU145 cells (*left*) and growth curve (*right*). **c**. Model. X and Y are different transcripts targeted by the same microRNA(s). In the steady state (*middle*), equilibrium exists between the microRNA molecules and their targets X and Y. Downregulation of X (*left*) leads to

increased availability of microRNA molecules to bind to Y, thus decreasing its abundance. By contrast, overexpression of X (*right*) leads to less microRNA molecules free to bind to Y, and thus Y abundance increases. Red rectangles: microRNA molecules. X and Y can be a pseudogene and its cognate protein-coding gene. **a** and **b.** mean ± s.d., n ≥ 3.